ELSEVIER

Journal of Alloys and Compounds 323–324 (2001) 86–90

Journal of ALLOYS AND COMPOUNDS

www.elsevier.com/locate/jallcom

# Transmission electron microscopy study of $Y_{1-x}\square_xCr_2S_4$, $x\sim1/3$ phase

A. Gómez-Herrero[a,*], A.R. Landa-Cánovas[a], A.W.S. Johnson[b], L.C. Otero-Díaz[a,c]

[a]*CME Luis Bru, Univ. Complutense de Madrid, Madrid, E-28040, Spain*
[b]*Electron Microscope Centre, University of Western Australia, Perth, Australia,*
[c]*Dpto. Química Inorgánica, Fac. CC. Químicas, Univ. Complutense de Madrid, Madrid, E-28040, Spain*

**Abstract**

A preliminary transmission electron microscopy study of the $YCr_3S_6$ phase has been performed. The compound crystallises with an orthorhombic average structure, space group *Pmnb*, $a=3.485$ (2) Å, $b=10.847$ (3) Å, $c=12.701$ (3) Å. The average crystal structure can be related to the **$CaFe_2O_4$-type**. In addition, the electron diffraction patterns show a three-fold superstructure along the *a* axis due to an ordered occupancy of the trigonal prismatic environment position by the yttrium atoms. In some cases it has been found that the modulation is slightly incommensurate. The presence of disorder giving rise to layers of diffuse intensity perpendicular to $a^*$ is related to the electron beam interaction as well as changes in the phase of the structure modulation. 

*Keywords:* Crystal structure and symmetry; Transmission electron microscopy; Order–disorder effects

## 1. Introduction

Ternary chalcogenides (X=S, Se, Te) made from rare earth ($Ln_2S_3$) and some transition (Cr, Mn, Fe) or alkaline (Mg, Ca, Sr) metals form a very large group of compounds that present a great interest to modern solid state physics and chemistry due to their many stoichiometries, structural variety and its associated properties, mainly magnetic and optical ones [1,2]. One of the most studied stoichiometries is $ALn_2X_4$, where A can be a first row transition metal or an alkaline earth metal. Hyde and Andersson [3] used the crystallographic operation of twinning at the unit cell level in order to describe some of those structures, thus when A is a small cation such as Mg, Mn, Cr and Ln is a heavy lanthanide, three structure types have been reported [3]: (i) **$CaTi_2O_4$-type**, a twinned ccp$\cdots$(4, 4)$\cdots$ anion array. A very deep TEM study of new phases related to this structure type has been done recently [4]. (ii) **$CaFe_2O_4$-type**, here the twinning is by glide reflection in a mixed hcp–ccp anion array. (iii) **$Yb_3S_4$-type**, related to the mineral warwickite, can be described as ribbons of edge sharing octahedra ($1\times4\times\infty$) occupied by $Yb^{3+}$ ions; the ribbons are joined by corner-sharing and related by glide reflection twinning [5].

For $Ln_2X_3$ compounds where Ln is a light lanthanide and $ALn_2X_4$ where A=Ca, Sr, Ba, the structure formed is **$Th_3P_4$-type**. In this structure the Th atoms are in eight coordinated positions inside distorted bisdisphenoids which share edges and faces [6,7].

More complex structures can also be formed when the transition metal is Ti, V or Cr. The prototype is the $\approx LaCrS_3$ ($La_{72}Cr_{60}S_{192}$) compound which has a semicommensurate misfit layer structure [8,9]. During the synthesis of the yttrium analogue compound, $\approx YCrS_3$, a phase with composition $\approx YCr_3S_6$ was formed. It is the purpose of this work to make a TEM characterisation of this phase.

## 2. Experimental methods

The sample was prepared by reaction of $Y_2S_3$ (prepared by sulphurization of $Y_2O_3$), Cr (5N) and S (5N) in a molar ratio of $Y_2S_3$:2 Cr:3S. The mixture of reactants was heated at 950°C during 7 days in an evacuated silica tube ($P\sim10^{-3}$ Torr). The product of this reaction was annealed at 1100°C in a new evacuated silica tube. The final product is a grey coloured microcrystalline powder.

The samples for the transmission electron microscopy (TEM) studies were ground under *n*-butanol and a drop of the suspension was left to evaporate on copper grids coated with holey carbon support film. A JEOL 2000FX electron microscope (double tilting $\pm45°$ holder) was used for the selected area electron diffraction (SAED) and convergent

*Corresponding author.

0925-8388/01/$ – see front matter 
PII: S0925-8388(01)00992-6

beam electron diffraction (CBED) studies. The crystals were analysed in the TEM by X-ray energy dispersive spectroscopy (XEDS) (Si(Li) detector, LINK ISIS 300 microanalysis system), the validity of the *k* factors used was checked by analysing several crystals of $Y_2S_3$ and $Cr_2S_3$. High resolution transmission electron microscopy (HRTEM) imaging was carried out using a JEOL 4000EX electron microscope (Cs=1.2 mm).

## 3. Results

The examination of the sample in the transmission electron microscope showed the presence of crystals with lamellar morphology and composition ~$YCrS_3$. Their SAED patterns showed unequivocally the characteristic features of the diffraction patterns of composite structures [8,9]: two sublattices of main reflections and satellite reflections due to the modulation of each subsystem by the another one and vice versa. The chemical composition and SAED data agree very well with the $(YS)_{1.28}CrS_2$ phase [10,11]. Besides, other crystals with composition ~$YCr_3S_6$ were also present as major constituent of the sample.

For an unknown phase it is possible to determine the Bravais lattice and the approximate unit cell parameters from a series of SAED patterns taken with a common row of reflections. The tilted angle between consecutive SAED patterns has to be measured from the goniometer readings in order to reconstruct the three-dimensional reciprocal lattice. By using this method, we have found for the ~$YCr_3S_6$ phase a primitive orthorhombic lattice with unit cell parameters: *a*~3.5 Å, *b*~10.8 Å, *c*~12.7 Å. In addition to this basic lattice, the SAED patterns (see Fig. 1) show weaker superlattice reflections which correspond to a three-fold superstructure along *a** with $a_s$~3×3.5 Å=10.5 Å. This data agree with the $YCr_3S_6$ phase firstly studied by Takahashi et al. [12] and Rustamov et al. [13], who synthesised different $LnCr_3S_6$ compounds and determined their unit cell parameters from X-ray diffraction data. However they did not carried out a microstructural study of these compounds.

The point group symmetry of the structure can be determined by analysis of the symmetry of microdiffraction and CBED patterns [14–17]. This symmetry together with the determination of extinction conditions can provide [14–20] a unique space group for the structure. Due mainly to the big unit cell parameters, i.e. to the close spacing between reflections, we have been obliged to use mainly the microdiffraction technique which requires more zone axes than CBED to determine the space group.

Figs. 2–4 show microdiffraction patterns of the ~$YCr_3S_6$ phase taken along the three main crystallographic directions. In order to show more clearly the whole pattern symmetry for every zone axis the crystal was slightly tilted away by rotating around every main row of reflections (*h00* or *0k0* or *00l*) to excite the high order Laue zones

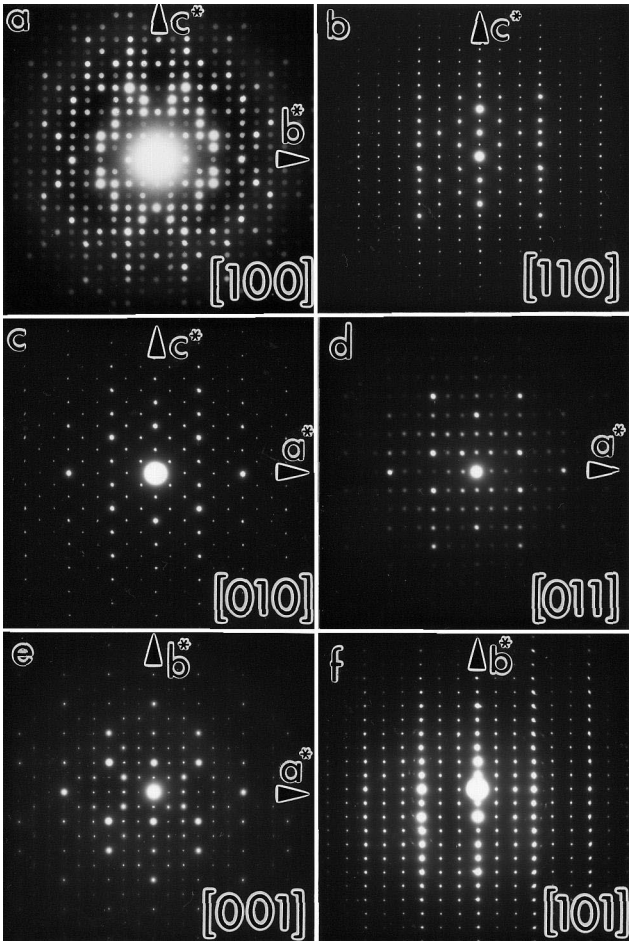


Fig. 1. (a–f) SAED patterns along the main zone axis of the $YCr_3S_6$ phase.

(HOLZ). This is important since the whole pattern (WP) symmetry of a microdiffraction pattern which shows HOLZ rings gives 3-dimensional information about the symmetry of the crystal. The WP symmetry for the basic sublattice is <u>*2mm*</u> for the three zone axis patterns, leading to a point group symmetry *mmm* for the sub-structure. The [100] zone axis (Fig. 2a) shows Gjønnes–Moodie lines along *b** and *c** in the *0k0:k=2n+1* and *00l:l=2n+1* reflections. The [010] zone axis (Fig. 3a) shows the complete absence of the reflections *h0l:h+l=2n+1* while the *h1l* reflections are visible in the first order Laue zone (FOLZ), see Fig. 3b,c. The extinction conditions for the basic substructure observed in Fig. 4a–c are more difficult to determine due to the strong interaction of the superlattice with the sublattice. Thus the *0k0:k=2n+1* forbidden reflections (see the Gjønnes–Moodie lines in Fig. 2a) are present due to the multiple diffraction of the superlattice reflections. Excluding these multiple diffraction reflections and paying attention only to the more intense substructure basic reflections the extinction condition deduced from this orientation is *hk0:k=2n+1.* Summarising, the observed extinction conditions for the average sublattice are then: *h0l:h+l=2n+1* and *hk0:k=2n+1.* They lead to the

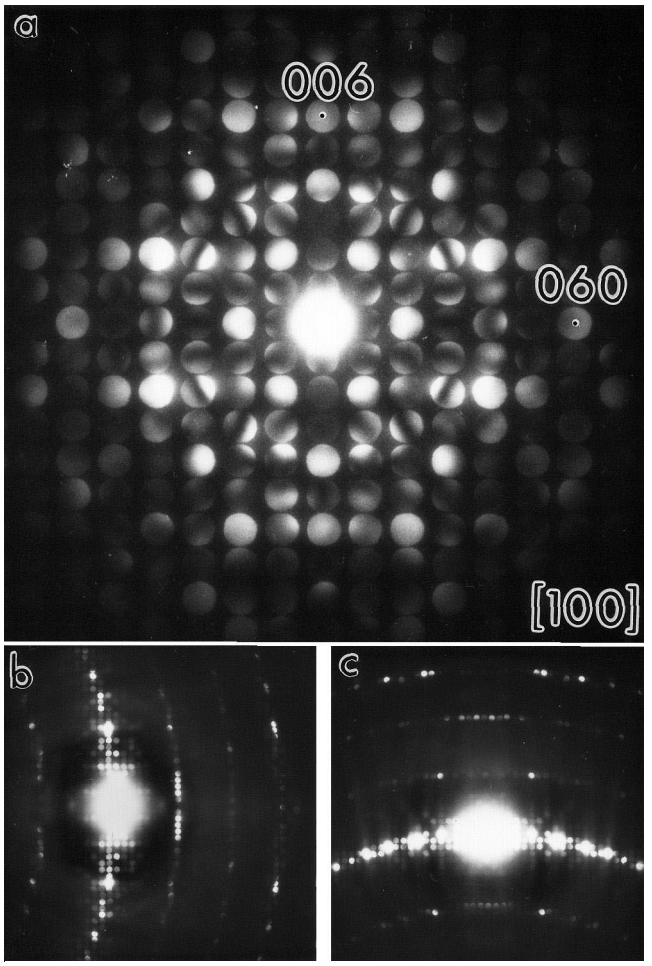


Fig. 2. (a) CBED pattern along [100]; (b, c) CBED patterns tilted away from [100] around [010]* and [001]* respectively.

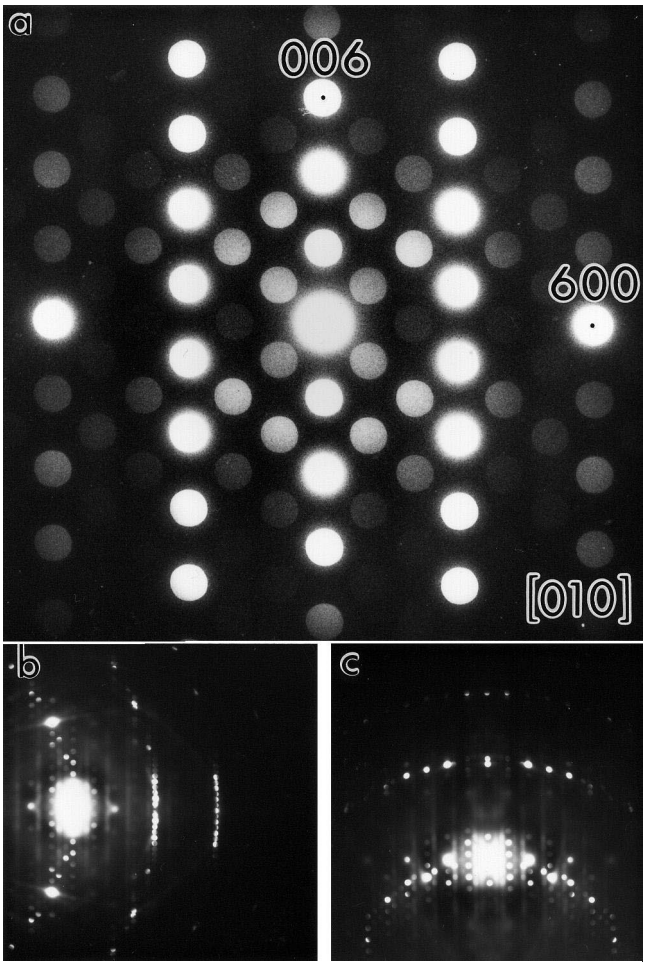


Fig. 3. (a) CBED pattern along [010] and off-tilted patterns.

extinction symbol *P–nb* [20], and together with the point group *mmm*, provide a *Pmnb* (no. 62) space group for the basic substructure with $a_{\text{basic}}=a/3\sim3.5$ Å.

The determination of the space group of the modulated structure became impracticable due to the nature of this modulation. Actually, from our TEM observations it does not seem correct to consider it as a three-fold superstructure but more as a structure modulation which sometimes is commensurate and sometimes slightly incommensurate, changing the position and amplitude of satellite reflections from crystal to crystal or even inside a particle. In Fig. 5 we show a SAED pattern where the splitting of some of the 'superlattice reflections' reveals the incommensurate nature of the structure modulation. Besides, we have some indications about a change of the modulation amplitude due to the electron beam interaction. Because of the need to use microdiffraction technique and of the orthorhombic symmetry of the crystals we need microdiffraction patterns along the three main zone axes which are 90° of tilting away from each other so it is impossible even to get two main zone axes from the same crystal. For all these reasons it has not been possible to determine the extinction conditions of the modulated structure. Moreover, the determined space group for the basic substructure is somewhat idealised considering no interaction between substructure and superstructure, mainly because of the WP symmetry observation along [001].

The superstructure unit cell parameters refined from the powder X-ray diffraction data are: $a=10.455$ (2) Å, $b=10.847$ (3) Å, $c=12.701$ (3) Å and the unit cell parameters of the basic substructure are then $a=3.485$ (2) Å, $b=10.847$ (3) Å, $c=12.701$ (3) Å. The SAED patterns of most of the crystals show different degrees of streaking running perpendicular to the $a^*$ axis through well defined satellite reflections, see Fig. 6. The tilting experiments reveal that this diffuse intensity corresponds to the intersection with the Ewald sphere of layers of diffuse scattering planes perpendicular to $a^*$. The layers are absent for the ($3h\ k\ l$) reciprocal planes of the basic sublattice. The coexistence of well defined satellite reflections and satellite planes of diffuse intensity can be explained by the presence of domains of well ordered material related by a shift

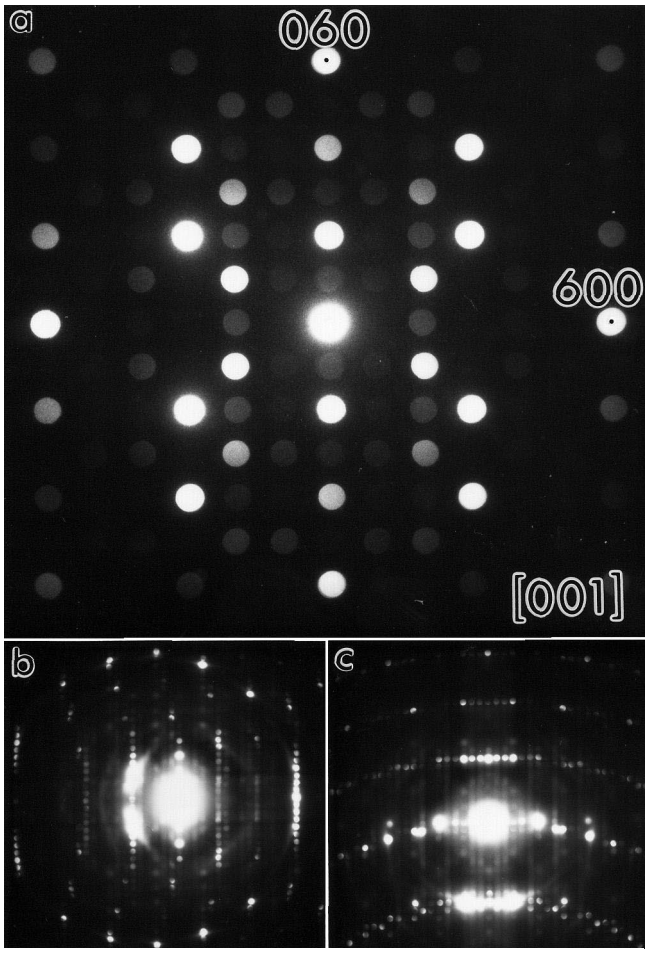


Fig. 4. (a) CBED pattern along [001] and off-tilted patterns.

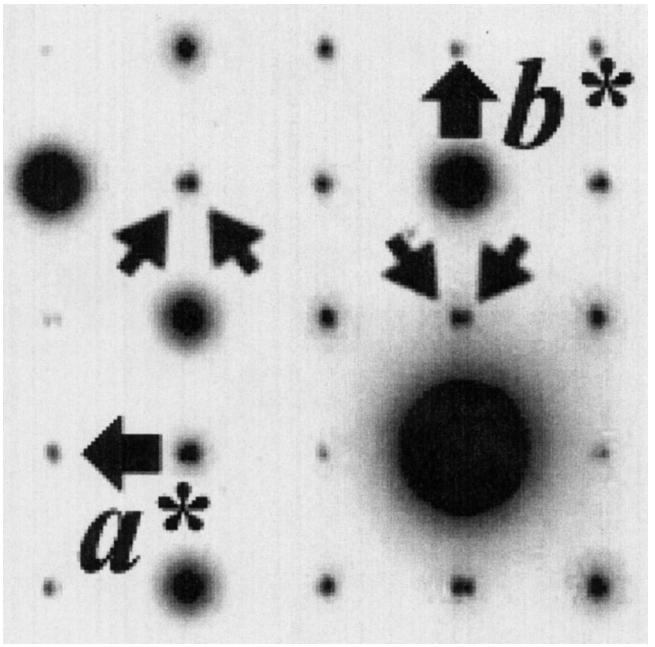


Fig. 5. Enlargement of a SAED pattern taken along [001], the splitting of the satellite reflections along $a^*$ indicates a deviation from the commensurate character of the structure.

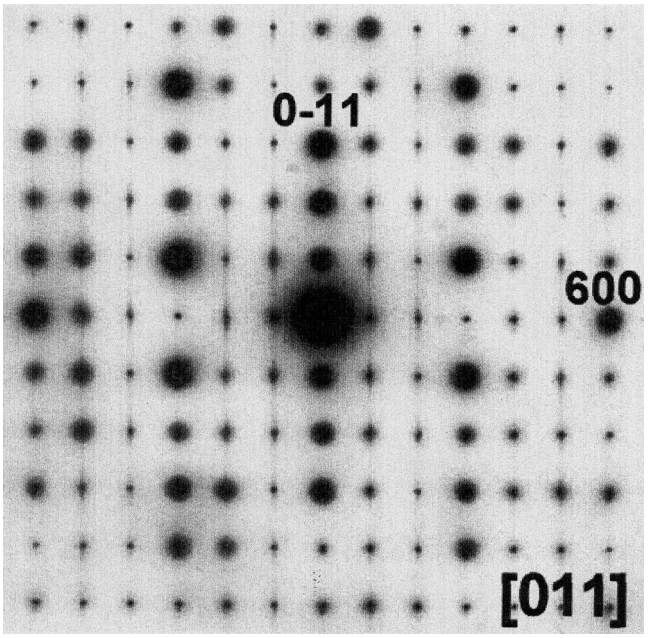


Fig. 6. SAED pattern showing streaking perpendicular to $a^*$ probably due to $a/3$ shifts in the atomic modulation wavefunctions.

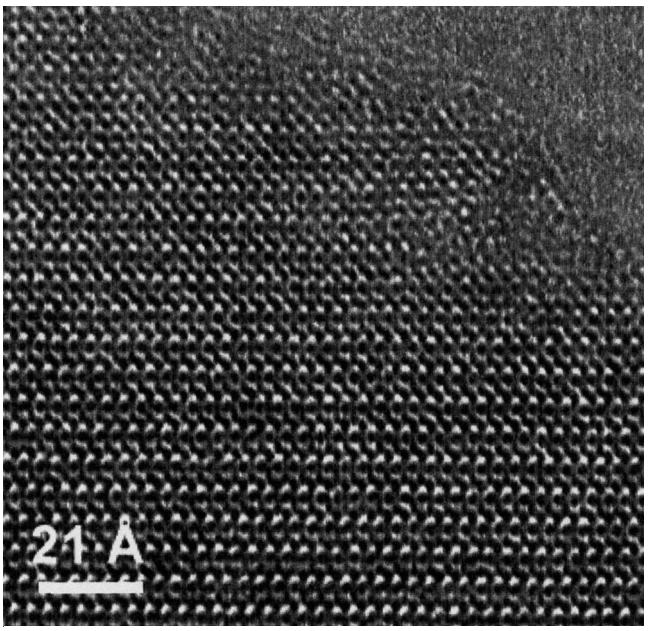


Fig. 7. HRTEM image of a crystal orientated along [010].

of $\pm 1/3\ a = a_{basic}$. High resolution micrographs taken at 400 kV, see Fig. 7, provide structural images at the atomic level resolution, but the crystals are very sensitive to the electron beam. The radiation damage is demonstrated by a increase of diffuse intensity between satellite reflections in the ED patterns. The superstructure finally disappears and the SAED patterns only show the basic reflections (see Fig. 8).

Our results show that $YCr_3S_6$ has an average structure

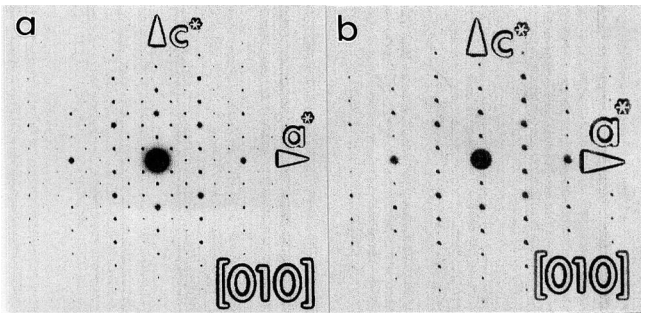


Fig. 8. (a) SAED pattern of one crystal of the $YCr_3S_6$ phase taken along [010] before; and (b) after irradiation with the 400 kV electron beam, note that the satellite reflections have vanished now when compared (a).

related to the **$CaFe_2O_4$ type** [3] (see Fig. 9), they also indicate that by analogy with $SmCr_3S_6$ and $GdCr_3S_6$ compounds [21,22], the structural modulation is originated by an ordered occupation along the *a* axis of the trigonal prism co-ordination polyhedra by the yttrium atoms: $Y_{2/3}\square_{1/3}Cr_2S_4 \equiv YCr_3S_6$. The mobility of the yttrium atoms in this trigonal prisms seems to be very high since the electron beam interaction breaks easily their order along *a** while the basic structure remains completely unaltered. Further work aims to study the superstructure behaviour of the superlattice reflections with the temperature: commensurate–incommensurate–disordered–random.

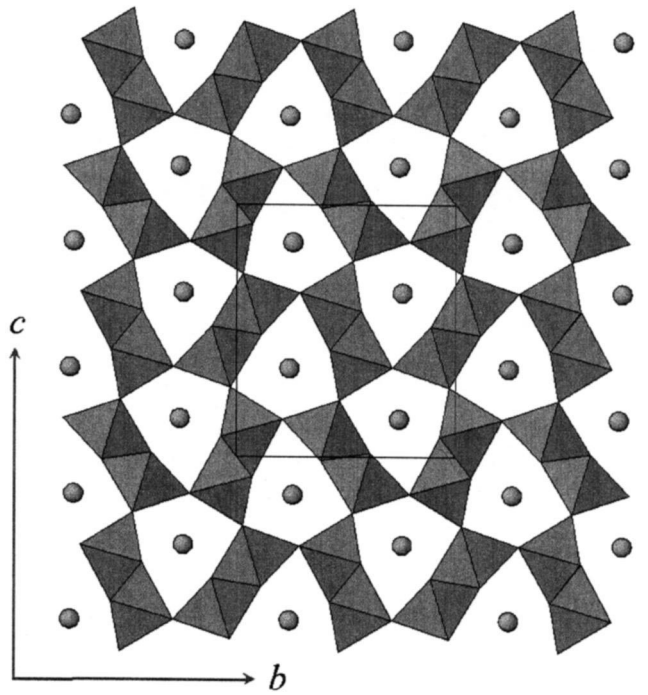


Fig. 9. The structure of $CaFe_2O_4$ projected along [100] in the non-standard *Pmnb* setting of space group *Pnma*.

## Acknowledgements

We wish to thank the financial support from CICYT research project MAT-97-0.697.CC01/02.0.

## References

[1] J. Flahaut, in: K.A. Gschneider Jr., L. Eyring (Eds.), Handbook on the Physics and Chemistry of Rare Earth, Vol. 4, North Holland, 1979, pp. 1–88.
[2] A.A. Eliseev, G.M. Kuzmichyeva, in: K.A. Gschneider Jr., L. Eyring (Eds.), Handbook on the Physics and Chemistry of Rare Earth, Vol. 13, North Holland, 1990, pp. 191–281.
[3] B.G. Hyde, S. Andersson, Inorganic Crystal Structures, J. Wiley, 1989.
[4] A.R. Landa-Cánovas, L.C. Otero-Díaz, Aust. J. Chem. 45 (1992) 1473–1487.
[5] L.C. Otero-Díaz, A.R. Landa-Cánovas, B.G. Hyde, J. Solid State Chem. 89 (1990) 237–259.
[6] J. Flahaut, M. Guittard, M. Patrie, M.P. Pardo, S.M. Golabi, L. Domange, Acta Cryst. 19 (1965) 14–19.
[7] H. Choi, C.H. Kim, C.H. Pynn, J. Solid State Chem. 131 (1997) 101–107.
[8] S. Kuypers, J. Van Landuyt, Materials Science Forum 100&101 (1992) 223–272.
[9] G.A. Wiegers, Prog. Solid State Chem. 24 (1996) 1–139.
[10] A. Lafond, C. Deudon, A. Meerschaut, A. Sulpice, Eur. J. Solid State Inorg. Chem. 31 (1994) 967–978.
[11] J. Rouxel, Y. Möelo, A. Lafond, F.J. DiSalvo, A. Meerschaut, R. Roesky, Inorg. Chem. 33 (1994) 3358–3363.
[12] T. Takahashi, K. Ametani, O. Yamada, J. Cryst. Growth 24/25 (1974) 151–153.
[13] P.G. Rustamov, T.Kh. Kurbanov, O.M. Aliev, I.P. Aliev, Izv. Akad. Nauk. SSSR, Neorg. Mater. 20 (1983) 1919–1921.
[14] A.R. Landa-Cánovas, L.C. Otero-Díaz, Difracción de electrones en el microscopio electrónico II: microdifracción y CBED, in: C.F. Hernández-Cano, C. Foces-Foces, M. Martínez-Ripoll (Eds.), Nuevas Tendencias, Vol. 26, Cristalografía, 1995, pp. 265–285.
[15] B.F. Buxton, J.A. Eades, J.W. Steeds, G.M. Rackham, Philos. Trans. R. Soc. London A281 (1976) 171–194.
[16] J.P. Morniroli, J.W. Steeds, Ultramicroscopy 45 (1992) 219–239.
[17] M. Tanaka, Acta Cryst. A50 (1994) 261–286.
[18] J. Gjønnes, A.F. Moodie, Acta Cryst. 19 (1965) 65–67.
[19] J.W. Steeds, R. Vincent, J. Appl. Cryst. 16 (1983) 317–324.
[20] A. Vos, M.J. Buerger, in: T. Hahn (Ed.), International Tables for Crystallography, Vol. A, Kluwer Acad. Publ, 1992, pp. 39–48.
[21] A. Meerschaut, A. Lafond, L.M. Hoistad, J. Rouxel, J. Solid State Chem. 111 (1994) 276–282.
[22] A. Lafond, L. Cario, A. Van der Lee, A. Meerschaut, J. Solid State Chem. 127 (1996) 295–301.